# GSA DATA REPOSITORY 2016201

# Supplemental Information for: Evidence for Cretaceous-Paleogene boundary bolide 'impact winter' conditions from New Jersey, USA

Johan Vellekoop*, Selen Esmeray-Senlet, Kenneth G. Miller, James V. Browning, Appy Sluijs, Bas van de Schootbrugge, Jaap S. Sinninghe Damsté, Henk Brinkhuis

*E-mail: johan.vellekoop@ees.kuleuven.be

This PDF file includes:
Materials and Methods
Text
References
Figs. DR1 to DR5
Tables DR1 to DR7

## Materials and Methods

1. Geological setting

The geology of the New Jersey coastal plain is characterized by Cretaceous, Paleogene and Neogene sediments deposited on the shelf of the western North Atlantic passive margin (Miller et al., 1998). The New Jersey shelf comprises a succession of mostly shallow marine deposits, ranging from the mid-Cretaceous up to the Miocene, with formations of different ages outcropping throughout the coastal plain (Miller et al., 1998). This succession has attained considerable attention, for example in terms of macrofossil studies (e.g., Landman et al., 2004), long-term sea-level reconstructions (e.g., Miller et al., 2005), and climate reconstructions (e.g., Sluijs et al., 2007; Van Helmond et al., 2013), involving studies on both outcrops and core material, both offshore (e.g. ODP Leg 150, ODP Leg 174A, IODP Expedition 313) as well as onshore (e.g. ODP Leg 150X, ODP Leg 174AX).

In the fall of 2008, Rutgers University commissioned the drilling of 14 additional, shallow (<25m) holes at 7 sites, to investigate the nature of the Cretaceous-Paleogene boundary in New Jersey (Miller et al., 2010). Drilling was done by United States Geological Survey (USGS) drillers, using a truck mounted Multi-twin G-30 Drill ("Sonic Metaprobe"). Of these cores, 3 were selected for the present study; Meirs Farm 1 (40°06'15.48" N, 74°31'37.48" W), Search Farm 1 (40°05'29.20" N, 74°32'16.10" W), and Fort Monmouth 3 (40°18'37.18' N, 74°02'46.25" W).

The Maastrichtian in the cores is characterized by grayish, bioturbated clayey glauconitic sands to glauconitic clays of the New Egypt Formation, superimposed by the heavily bioturbated clayey glauconitic sands of the Danian Hornerstown Formation (Miller et

al., 2010). The K-Pg boundary is marked by a 3-5 cm thick layer of white clay,, containing uppermost Cretaceous foraminifera and dinocysts. This distinctive layer has been interpreted as deposited by a tsunami, triggered by slope failure on the US east coast due to earthquakes generated by the Chicxulub impact (Olsson et al., 2002; Miller et al., 2010). In the Meirs Farm core a 5-cm-thick white clay layer, comprised of siderite, possibly representing a weathered carbonate spherules and/or carbonate accretionary lapilli (Yancey and Guillemette, 2008), is overlain by gray, burrowed glauconitic sands, with above this a transition to green, heavily bioturbated glauconitic sands. In the Search Farm and Fort Monmouth 3 cores, the K-Pg boundary is directly overlain by the green glauconitic sands. For precise locations and a more detailed description of these cores, lithologies, including adjacent outcrops, see Miller et al. (2010). These cores were sampled and processed for palynology, planktic foraminifera, and Iridium to generate an age model and for organic geochemistry to quantitatively portray long and short-term SST changes across the K-Pg boundary.

2. Organic-walled dinoflagellate cysts

In total, 65 samples were processed for palynological analyses following standard palynological preparation techniques of the Laboratory of Palynology and Palaeobotany, see Açikalin et al. (2015) for a more detailed description. All slides are stored in the collection of the Laboratory of Palaeobotany and Palynology, Utrecht University. For each sample, dinocysts were counted up to a minimum of 200 specimens. The taxonomy of dinocysts follows that cited in Fensome and Williams (2004) unless stated otherwise (see Supplementary Information, Tables and Figures: 3. Taxonomy).

3. Planktic foraminifera

The Fort Monmouth 3 core was analyzed for planktic foraminifera. In total, 13 samples were disintegrated using Calgon solution (5.5 g of sodium metaphosphate per one liter of water) and washed with tap water through a 63-μm sieve. After being dried in an oven at 40°C, samples were sieved through 250, 150, 125, and 63 μm sieves. Representatives of individual species were picked from the various size fractions and stored in slides. Planktic foraminiferal identifications follow the taxonomy of Premoli Silva and Verga (2004) for the Cretaceous and Olsson et al. (1999) for the Paleocene.

4. Iridium analysis

Iridium analyses have previously been performed on the K-Pg boundary interval of the Meirs Farm and Search Farm cores, showing an Ir anomaly characteristic for the K-Pg boundary layer (Miller et al., 2010). The lithology suggests that at the Fort Monmouth 3 core the K-Pg boundary layer is missing (see Supplementary Information, Tables and Figures: 1. Lithology of the K-Pg boundary interval). To confirm this, we analyzed 16 additional samples from the K-Pg boundary interval of the Fort Monmouth 3 core for Ir. Concentrations of Ir were measured with high sensitivity Sector Field Inductively Coupled Plasma Mass Spectrometry at the Department of Marine and Coastal Sciences, Rutgers University with detection limits of 0.01 ppb. For the ICP-MS measurements preconcentration of Ir from sediments were done by NiS fire-assay technique modified after Ravizza and Pyle (1997). In this method 1-1.5 g of sample is ground to a powder and homogenized, then mixed with NiS (2:1 ratio of Ni:S), borax (2:1 ratio of borax to sediment mass) and $^{191}$Ir enriched isotope spike prepared in 6.2N HCl. This mixture is then heated to 1000°C for 75 minutes to allow fusion. After fusion process, beads obtained are dissolved on 190- 200°C hot plates, filtered and filters are digested.

5. Organic geochemical analysis

In total, 58 aliquot samples were investigated for the determination of $TEX_{86}$ and BIT indices following standard procedures (e.g. Schouten et al., 2007). Briefly, we extracted glycerol dialkyl glycerol tetraethers (GDGTs) using organic solvents and quantified the various GDGTs using high performance liquid chromatography/atmospheric pressure positive ion chemical ionization mass spectrometry (HPLC/ APCI-MS; Schouten et al., 2007). Since we apply the $TEX_{86}$ paleothermometer on samples from a mid-latitude site from a Cretaceous-Paleogene greenhouse world, unambiguously characterized by high Sea Surface Temperatures (SSTs) (>$15^0$C), we applied the calibration from Kim et al. (2010) to calculate mean annual sea surface temperature. The branched and isoprenoid tetraether (BIT) index, indicative for the relative input of soil-derived organic matter, was calculated following Hopmans et al. (2004). Samples with BIT index values of >0.3 were discarded, since this may indicate elevated input of isoprenoid GDGTs from soil organic matter, obscuring $TEX_{86}$ paleothermometry (Weijers et al., 2006). Five of the analyzed samples were run in duplicate, the reproducibility is better than 0.5 °C, and in most cases better than 0.25 °C. The residual standard error for the calibration model is 2.5 °C (Kim et al., 2010). In the case where all analyses are from one site this should be considered as a potential systematic error that may shift all data points of a record in one direction.

## Supplementary Information

1. Lithology of the K-Pg boundary interval

At the New Jersey coastal plain, Maastrichtian and Paleocene deposits encompass 6 formations: the Navesink, New Egypt, Red Bank, Tinton, Hornerstown and Vincentown formations (Minard, 1969). The Maastrichtian Navesink Formation consists of burrow-mottled, glauconitic, clayey sand to sandy clays and the upper Maastrichtian Red bank and Tinton formations consist of micaceous, silty, fine grained, feldspathic quartz sand and glauconitic quartz sand, respectively, interpreted to be deposited in an inner shelf environment (Olsson, 1987; Landman et al., 2004). The upper Maastrichtian New Egypt Formation, consisting of dark gray, glauconitic, clayey sand to sandy clay, is the down-dip equivalent of the Red Bank and Tinton formations, representing a deeper-water facies of these units (Olsson, 1987; Landman et al., 2004). In all 3 cores selected for the current study, the uppermost Maastrichtian is represented by this deeper-water facies. Both the Tinton Formation and New Egypt Formation are overlain by the lower Paleocene Hornerstown Formation, consisting of green, burrow-mottled, glauconitic clayey sand to micaceous, quartzose, glauconite sand (Minard, 1969; Olsson, 1987; Landman et al., 2004). The abundant glauconite results in a dark greenish color, giving the formation its informal name of ‘‘Greensand Marl’’ (Landman et al., 2004). At most localities on the New Jersey coastal plain, the contact between the Tinton/New Egypt formations and Hornerstown Formation marks the K-Pg boundary. In New Jersey records that are stratigraphically more complete, the K-Pg boundary is marked by a 3-5 cm thick layer of white clay, containing uppermost Cretaceous foraminifera and dinocysts (Olsson et al., 2002; Miller et al., 2010), with, even further downdip, such as at Bass River (Ocean Drilling Program Leg 174AX), also a spherule bed (Olsson et al., 1997). The distinctive white clay layer has been interpreted as rip-up clasts deposited by a tsunami, triggered by slope failure on the US east coast due to earthquakes generated by the Chicxulub impact (Olsson et al., 2002; Miller et al., 2010), but might also represent weathered carbonate accretionary lapilli (Yancey and Guillemette, 2008). In the Meirs Farm core, the white clay layer is overlain by ~60 cm of grayish, bioturbated clayey glauconitic sand, similar to that of the underlying New Egypt Formation. Above this is the transition to the green, heavily bioturbated glauconitic sands of the Hornerstown Formation (See Fig. DR1). In the Search Farm and Fort Monmouth 3 cores, the K-Pg boundary is directly overlain by the green glauconitic sands of the Hornerstown Formation. In the Search Farm core, the remnants of the white clay clast layer are still visible at the highly burrowed, unconformable contact between the New Egypt and Hornerstown formations, whereas at the Fort Monmouth 3 core, no white clay clasts were observed, suggesting that there, the boundary layer is missing in this core.

Across the New Jersey coastal plain, the Hornerstown varies in thickness, form 1.5 m up to >10m.

2. Preservation

The three cores were sampled in high resolution and analyzed for organic-walled dinoflagellate cysts, planktic foraminifera and $TEX_{86}$ paleothermometry (See SI Tables 1-4). Samples from the New Egypt Formation are generally characterized by excellent preservation of organic material (dinocysts and GDGTs). The basal part of the Hornerstown Formation, consisting of green, intensely burrowed glauconitic sands, is, on the other hand, characterized by poor preservation of organic material, obscuring application of the organic biomarker-based $TEX_{86}$ paleothermometry and palynological analyses in this interval.

The Meirs Farm and Search Farm cores are characterized by poor carbonate preservation, not permitting planktic foraminiferal biostratigraphy. The Fort Monmouth 3 core comprised sufficient foraminifera to allow planktic foraminiferal biostratigraphy.

3. Taxonomy

The taxonomy of dinocysts follows that cited in Fensome and Williams (2004). A few divergent opinions, however, are listed below.

*Damassadinium* cf. *californicum* (Drugg 1967) Fensome et al. 1993

Remarks: This species of *Damassadinium* occurs in pPlanktic foraminiferal Zones P0 and Pα, and shows resemblances to *D. californicum*, but distinguished from it by having a less broad process base. In this study, this morphotype is regarded as a predecessor for *Damassadinium californicum* s.s.

*Disphaerogena carposphaeropsis* var. *cornuta* nov. var.

Remarks: This variety of *Disphaerogena carposphaeropsis* occurs in in the uppermost Maastrichtian and lower Danian, with its first occurrence roughly at the base of the uppermost Maastrichtian *M. prinssii* Zone. This variety closely resembles *D. carposphaeropsis* s.s., but is distinguished from it by alarge antapical horn. According to the emended diagnosis of Sarjeant, 1985, *Disphaerogena carposphaeropsis* s.s is characterized by an apical horn that is always longer than the antapical horn, by a ratio varying between 1.2:1 to 3:1. In the uppermost Maastrichtian samples, specimen occur with an antapical horn that is as long as, or longer than the apical horn. Since this form first appears in the uppermost Maastrichtian (i.e. Vellekoop et al., 2014, Açikalin et al., 2015), it is used as a stratigraphic marker in the present study. Since this form clearly belongs to the species *D. carposphaeropsis*, but is characterized by an antapical horn similar to the taxon *Carpatella cornuta*, we used the informal name '*Disphaerogena carposphaeropsis* variety "*cornuta*"' in study, after its characteristic horns.

*Senoniasphaera* cf. *inornata* (Drugg 1970) Stover and Evitt 1978

Remarks: This species of *Senoniasphaera* occurs at the base of planktic Foraminiferal Zones P0, and shows a resemblance to *S. inornata*. It is distinguished from it by having a smaller size and thinner outer wall. In this study this morphotype is regarded as a predecessor for *Senoniasphaera inornata* s.s.

Planktic foraminifera identifications follow the taxonomy of Premoli Silva and Verga (2004) for the Cretaceous and Olsson et al. (1999) for the Paleocene.

4. Age model

4.1. Fecal pellets and iridium

The age model of the studied cores is based on the presence of impact derived iridium (Miller et al., 2010 and this study) and planktic foraminiferal and dinocyst biostratigraphy (this study). In addition, the appearance of a distinct level with abundant echinoid fecal pellets can be used as a distinctive marker for the lowermost Danian in New Jersey (Miller et al., 2010) (see Fig. DR2.). The abundant presence of fecal pellets of epifaunal echinoids in this interval is likely related to the dramatic decrease in export production following the K-Pg boundary extinction event, which resulted in increased benthic bulldozing (Miller et al.,

2010). Our iridium analysis of the Fort Monmouth 3 core shows that no iridium anomaly is present, confirming that there, the K-Pg boundary layer is missing (Fig. DR3.).

4.2. Dinocyst biostratigraphy

Dinocyst biostratigraphy allows for a detailed control for both the Maastrichtian and Danian. See SI Tables 5-8 for an overview of ranges of dinocyst marker taxa. Of the four studied cores, the Meirs Farm core ranges furthest down into the Maastrichtian. This core comprises the First Occurences (FOs) of the dinocyst marker taxa *Palynodinium grallator* and *Disphaerogena carposphaeropsis*, which have their First Appearance Datum (FAD) at approximately 67 Ma (15, 52). In the upper Maastrichtian of the Meirs Farm, Search Farm and Fort Monmouth 3 cores, the FO's of *Manumiella seelandica* and *Thalassiphora pelagica* are observed. In addition, these records show an acme of the marker taxa *P. grallator*. This acme is very characteristic for the topmost Maastrichtian *T. pelagica* Subzone of the boreal realm, as described by Hansen et al. (1977) and Schiøler and Wilson (1993) for the North Sea basin, also being recognized in for example the North Sea wells (Schiøler and Wilson, 1993) and Southern Sweden (Hultberg and Malmgren, 1987).

The Danian interval of the studied cores shows a succession of dinocyst marker taxa. The Meirs Farm core includes the successive FOs of the lowermost Danian markers *Senoniasphaera* cf. *inornata* and *Membranilarnacia*? *tenella* and *Damassadinium* cf. *californicum*. Because the range of the characteristic dinocyst taxon *Senoniasphaera* cf. *inornata* is restricted to planktic foraminiferal Zone P0 (Vellekoop et al., 2014; Açikalin et al., 2015), the presence of this marker taxon indicates that the equivalent of planktic foraminiferal Zone P0 is present at present at the Meirs Farm core. The taxon *S.* cf. *inornata* was not encountered at Search Farm and Fort Monmouth 3, suggesting that the lowermost Danian was not preserved in these cores. In Meirs Farm, Search Farm and Fort Monmouth 3, the basal part of the Hornerstown Formation comprises the FOs characteristic early Danian marker taxa *Damassadinium californicum* and *Carpatella cornuta* (Fig. DR2.). These results show that at the Meirs Farm core the K-Pg boundary interval is most complete, whereas the boundary interval at the Search Farm and Fort Monmouth 3 cores is characterized by a short hiatus or a condensed interval.

4.3. Planktic foraminiferal biostratigraphy

The Meirs Farm 1 and Search Farm 1 cores were barren of planktic foraminifera, but the Fort Monmouth 3 core was productive, allowing us to construct planktic foraminiferal biostratigraphy. See SI Tables 9 and 10 for an overview of ranges of planktic foraminiferal marker taxa. The Maastrichtian interval is dominated by typical shallow marine uppermost Cretaceous planktic taxa like *Heterohelix globulosa*, *H. navarroensis*, *Guembelitria cretacea*, *Globigerinelloides messinae*, and *G. praiehillensis*. There are no keeled species present in the samples and uncoiled forms are more abundant than coiled forms. Since keeled taxa were not encountered, the keeled uppermost Maastrichtian marker taxon *Abathomphalus mayaroensis* is also absent. This planktic species likely developed its adult morphology in the deeper part of the water column and is therefore probably not present at these sites characterized by very shallow paleodepths (Miller et al., 1998). The dominance of *Heterohelix* is typical for Late Maastrichitan shallow marine sites (Pardo and Keller, 2008). The presence of these other planktic foraminifera and dinocyst taxa characteristic for the uppermost Maastrichtian, such as *G. messinae*, *D. carposphaeropsis*, *P. grallator* and *T. pelagica* indicate that the studied part of the New Egypt Formation is equivalent to the *Pg. hariaensis/Pl. hantkeninoides* Zone,

allowing us to tentatively assign this interval, using an approach similar to ref. (Miller et al., 1998).

In the Fort Monmouth 3 core, foraminifera are very scarce above the K-Pg boundary, with only rare specimens of *Heterohelix* present. At 15.1 mbls, the assemblage is dominated by *G. cretacea*. This survivor species of the K-Pg mass extinction commonly forms an acme in the earliest Danian (Brinkhuis and Zachariasse, 1988). In this sample the Cretaceous taxa *H. globulosa*, *H. navarroensis*, and *Globigerinelloides* spp. are also present. The high abundance of *G. cretacea*, the survivor species of the K-Pg mass extinction commonly forming an acme zone in the early Danian, suggests that these Cretaceous forms represent reworked specimens. These analyses suggest that at the Fort Monmouth 3 core, the basal part of the Hornerstown Formation is correlative to planktic foraminiferal zones P0 or Pα (Olsson et al., 1999).

4.4. Summary of biostratigraphy

Dinocyst biostratigraphy allows an excellent age control for both the Maastrichtian and Danian parts of the cores (See Fig. DR2). Of the four studied cores, the Meirs Farm core ranges furthest down into the Maastrichtian. This core comprises the First Occurences (FOs) of the dinocyst marker taxa *Palynodinium grallator* and *Disphaerogena carposphaeropsis*, that have their First Appearance Datum (FAD) at ~67 Ma (DeGracianski et al., 1998; Williams et al., 2004) and are representative of the uppermost Maastrichtian *P. grallator* Zone of Hanssen (1977). The FO of the marker taxon *T. pelagica* allows the subdivision of the *P. grallator* Zone into the *T. magdalium* and *T. pelagica* Subzones (Hanssen, 1977).

In the earliest Danian interval, the characteristic early Danian marker taxa *Senoniasphaera* cf. *inornata*; *Senoniasphaera inornata*, *Damassadinium californicum* and *Carpatella cornuta* are successively encountered (Figs. DR2 and DR3), with respective FADs at approximately ~66.04, ~66.00, ~65.75 and ~65.7 Ma (Brinkhuis et al., 1998; Williams et al., 2004; Vellekoop et al., 2014).

Carbonate preservation is poor for the Maastrichtian interval of our cores. The Meirs Farm 1 and Search Farm 1 cores were barren in terms of planktic foraminifera, but the Fort Monmouth 1 and 3 cores comprised sufficient foraminifera to allow us to also construct a planktic foraminiferal biostratigraphy. Plankic foraminiferal analysis indicates the presence of zones P0/ Pα, (Olsson et al., 1999). Therefore, our combined records indicate that the resulting composite section ranges in age from approximately 1.1 million years before the K-Pg boundary up to approximately ~100 kyrs after the boundary, using the absolute ages derived from Gradstein et al. (2012).

5. Correlation of the cores

Our detailed litho- and biostratigraphy allows a correlation between the four studied cores (see Fig. DR3). The Meirs Farm core ranges furthest down into the Maastrichtian, comprising the FOs of *P. grallator* and *D. carposphaeropsis*. These taxa are already present at the base of the Search Farm and Fort Monmouth 3 cores. The top part of the New Egypt Formation is equivalent to the *Pg. hariaensis/Pl. hantkeninoides* Zone and is characterized by the FOs of *T. pelagica* and *M. seelandica* and by the acme of *P. grallator*. These bio-events are characteristic for the uppermost Maastrichtian *T. pelagica* Subzone and can be used to correlate the uppermost Maastrichtian interval between the cores. Based on this correlation it is evident that the topmost Maastrichtian is slightly more condensed at the Search Farm and Fort Monmouth 3 cores.

A distinctive white clay layer marking the K-Pg boundary is best preserved in the Meirs Farm core. Though labeled as a clast by Miller et al. (2010), examination of adjacent outrcrops suggest that this is actually a an altered white clay comprised of siderite that is 3-5 cm thick.. The basal part of the HornerstownFm comprises the subsequent FOs of the characteristic lowermost Danian dinocyst marker taxa *S.* cf. *inornata*, *M.*? *tenella*, *S. inornata*, *D.* cf. *californicum*, suggesting that this interval is equivalent to Planktic Foraminiferal Zone P0 and the basal part of Zone Pα (Vellekoop et al., 2014; Açikalin et al., 2015).

At the Search Farm and Fort Monmouth 3 cores, the K-Pg boundary is marked by the base of the Hornerstown Fm, which comprises the FO's of the Danian dinocyst marker taxa *D. californicum* and *C. cornuta* and the Danian planktic foraminiferal marker taxa *G daubjergensis* and *W. claytonensis*, indicating that this base is equivalent to planktic foraminiferal Zone Pα. At the highly burrowed, unconformable contact between the New Egypt and Hornerstown Fms of the Search Farm core, the remnants of the white clay clast layer are visible and a small iridium anomaly was encountered. At the Fort Monmouth 3 core, no iridium anomaly or white clay clasts were encountered at the contact between the New Egypt and Hornerstown Fms. This indicates that at Fort Monmouth the K-Pg boundary layer is missing at this core. Based on the position of the acme of *P. grallator*, we estimate that the top ~50 cm of the Maastrichtian have probably also been eroded away at this core.

With these correlation possibilities, a composite (splice) can be constructed using the four studied cores (Fig. 2.).

The splice of the cores investigated in this study can in turn be correlated to the nearby Bass River core (ODP Leg 174AX) (Fig. 3.). The Bass River locality is approximately 60 km South of the drill site of the Meirs Farm core (Fig. 1.) and represents a more offshore site, relatively to the cores investigated in this study (Esmeray-Senlet et al., 2015). A biostratigraphic correlation between the Bass River core and the splice of cores investigated in this study is difficult, because nannofossil and planktic foraminiferal zonations are absent for the cores of our study and a dinocyst zonation is absent for the Maastrichtian part of Bass River. Since the New Egypt and Hornerstow formations are represented at both sites, a lithostratigraphic correlation is possible. The New Egypt Fm is much more expanded at Meirs Farm (>9m) compared to Bass River (3-5m) (Fig. 3.), suggesting that the uppermost Maastrichtian is more expanded in the cores studied here.

Interestingly, the $TEX_{86}$ records of the splice of cores investigated in this study shows a very similar pattern to the $\delta^{18}O$ records of Bass River (Olsson et al., 2001; Olsson et al., 2002; Esmeray-Senlet et al., 2015). Therefore, the temperature records provide have a correlative power on their own (Fig. 3.). The late Maastrichtian warming event possibly reflects an episode of global greenhouse warming, which is also documented for example by poleward migration of warm-water planktic foraminifera (Kucera and Malmgren, 1998). Perhaps this warming phase is related to the second major outpouring phase of the Deccan traps. This onset of this major outpouring phase is dated at 66.288 ± 0.027/0.047/0.085 Ma (Schoene et al., 2015), starting after the C30n/C29r magnetic reversal (Ravizza and Peucker-Ehrenbrink, 2003; Robinson et al., 2009), in line with our biostratigraphic age model.

## 6. $TEX_{86}$ paleothermometry

In the samples analyzed for this study, concentrations of isoprenoidal GDGTs range from 5-80 ng/g dry-weight sediment. The overall chromatography of the GDGTs was excellent, with proper signal to noise ratios.

In recent years, it has been shown that $TEX_{86}$-inferred temperatures can deviate significantly from actual temperatures, depending on environmental conditions and archeal

community composition. The reconstructed absolute temperatures should thus be interpreted with care (see Materials and Methods 5. Organic geochemical analysis). Here we nevertheless predominantly aim to reconstruct trends i.e. changes in SST rather than absolute temperatures. While $TEX_{86}$ is calibrated to SST (Schouten et al., 2002), various studies suggested $TEX_{86}$ might sometimes reflect deeper water temperatures (e.g., Huguet et al., 2007; Lopes dos Santos et al., 2010). However, the studied sedimentary succession was deposited at a shallow, shelf depositional environment (water depth of <35 m; Miller et al., 2010; Esmeray-Senlet et al., 2015), excluding the possibility that the recorded temperature trends would significantly differ from trends in SST.

High concentrations of Soil Organic Matter (SOM) in sediments may cause a bias in $TEX_{86}$-reconstructed sea surface temperatures (Weijers et al., 2006). The relative amount of SOM in sediments can be approximated based on the analysis of tetraether lipids, using the so-called Branched and Isoprenoid Tetraether (BIT) index (Hopmans et al., 2004). To identify whether our $TEX_{86}$ record is biased by the input of SOM, we calculated the BIT index for all our samples. To exclude all $TEX_{86}$-reconstructed sea surface temperatures possibly biased by high concentrations of terrestrial-derived GDGTs, we discarded samples with a BIT-index exceeding the recommended (Weijers et al., 2006) threshold of 0.3 (4 out of 55 analyzed samples; see Fig. DR4.).

A possible bias in $TEX_{86}$ palaeothermometry may also be introduced by the input of methanogenic and methanotrophic archaeal GDGTs, leading to erroneous SST reconstructions (Blaga et al., 2009; Weijers et al., 2011; Zhang et al., 2011). Potential contribution of methanogenic and methanotrophic archaeal GDGTs can be recognized using the ratio of GDGT-0/Crenarchaeol (Blaga et al., 2009) and the Methane Index (Zhang et al., 2011), respectively. In our study, the GDGT-0/crenarchaeol ratio ranges between 0.21 - 1.28, well below the recommended threshold of 2.0 (Blaga et al., 2009), whereas the Methane Index ranges between 0.19-0.29, below the recommended threshold of 0.5 (Zhang et al., 2011) (Fig. DR5). These values suggest that at the studied locality there is little to no input of GDGTs derived from methanogenic or methanotrophic archaea.

The cultivation experiments of Qin et al. (2015) have shown that variations oxygen limitation can also result in large deviations in reconstructed temperatures. Hence, $TEX_{86}$ results should be interpreted with caution in records that span low-oxygen events or underlie oxygen minimum zones. Fortunately, our records from the New Jersey paleo shelf represent a very shallow marine, well-oxygenated environment (e.g. Miller et al., 2010; Esmeray-Senlet et al., 2015), indicating that oxygen limitation played no role in these records.

As the K-Pg boundary bolide impact resulted in a mass-extinction event (Schulte et al., 2010), it is possible that this boundary is also characterized by large changes in microbial community composition, possibly affecting the $TEX_{86}$ signal (Qin et al., 2015). Ammonium-oxidizing archaea are nonetheless known to have a wide habitat range, suggesting both high ecotypic diversity and adaptive capacity (Qin et al., 2014; Martens-Habbena et al., 2009). These characteristics arguably make this biological group less susceptible to extinction events. Furthermore, Thaumarchaeota have been shown to be able to grow chemoautotrophically in complete darkness (Wuchter et al., 2004). It therefore seems unlikely that the darkness during the K-Pg boundary impact winter, suggested to have been the main driver for the K-Pg boundary mass extinction (Alvarez et al., 1980), will have resulted in significant extinctions among the thaumarchaeotal community. This suggests that the $TEX_{86}$ palaeothermometry can be applied with relative confidence across the K-Pg boundary interval in the present record. Organic temperature proxies may also be affected by vital effects. For example, studies on $TEX_{86}$ in thaumarchaeotal enrichment cultures (Wuchter et al., 2004;

Schouten et al., 2007; Qin et al.) revealed that the temperature response was different from that based on the global core top calibrations. For all these studies, it should be realized, however, that the sedimentary signal of organic molecules reflects the average biological response of many species that contribute and, in this respect, should be considered as a "system" response. Although culture studies are very useful in understanding the mechanisms of membrane lipid adaptation in microbes, it remains a challenge to directly "translate" these to the interpretation of proxy records.

# References


Blaga, C.I., Reichart, G.J., Heiri, O., Sinninghe Damsté, J. S., Tetraether membrane lipid distributions in lake particulate matter and sediments: A study of 47 European lakes along a North-South transect. Journal of Paleolimnology 41, 523–540 (2009).

Brinkhuis, H., Zachariasse, W.J., 1988. Dinoflagellate cysts, sea level changes and planktonic foraminifers across the Cretaceous-Tertiary boundary at El Haria, northwest Tunisia. Marine Micropaleontology 13, 153-191.

De Gracianski, P. C., Hardenbol, J., Jacquin, T., Vail, P. R., 1998. Mesozoic–Cenozoic Sequence Stratigraphy of European Basins. Society of Economic Paleontologists and Mineralogists Special Publication, SEPM, Tulsa, OK, Vol. 60, 786pp.

Fensome, R. A., Williams, G. L., 2004. The Lentin and Williams Index of Fossil Dinoflagellages 2004 edition. American Association of Stratigraphic Palynologists Foundation Contr. Series.

Heilmann-Clausen, C., 1985. Dinoflagellate stratigraphy of the uppermost Danian to Ypresian in the Viborg I borehole, central Jylland, Denmark. Danmarks Geologiske Undersøgelse, Serie A, no.7, 1-69, pl.1-15.

Hopmans E. C., Weijers, J. W. H., Schefuss, E., Herfort, L., Sinninghe Damsté, J. S., Schouten, S., 2004. A novel proxy for terrestrial organic matter in sediments based on branched and isoprenoid tetraether lipids: Earth and Planetary Science Letters 224, 107-116.

Huguet, C., Schimmelmann, A., Thunell, R., Lourens, L. J., Sinninghe Damsté, J. S., Schouten, S., 2007. A study of the $TEX_{86}$ paleothermometer in the water column and sediments of the Santa Barbara Basin, California: Paleoceanography 22, PA3203. DOI: 10.1029/2006PA001310

Hultberg, S.U., Malmgren B.A., 1987. Quantitative biostratigraphy based on Late Maastrichtian dinoflagellates and planktonic foraminifera from Southern Scandinavia. Cretaceous Res., 8:211-228.

Kucera, M., Malmgren, B.A., 1998. Terminal Cretaceous warming event in the mid-latitude South Atlantic Ocean: evidence from poleward migration of *Contusotruncana contuse* (planktonic foraminifera) morphotypes: Palaeogeography, Palaeoclimatology, Palaeoecology 138, 1-15.

Landman, N. H., Johnson, R. O., Edwards, L. E., 2004. Cephalopods from the Cretaceous-Tertiary boundary interval on the Atlantic coastal plain, with a description of the highest ammonite zones in North Amercia. Part 2. Northeastern Monmouth County, New Jersey. Bulletin of the American Museum of Natural History 287, 1-107. DOI: 10.1206/0003-0090(2004)287<0001:CFTTBI>2.0.CO;2

Lopes dos Santos, R., Prange, M., Castañeda, I.S., Schefuß, E., Mulitza, S., Schulz, M., Niedermeyer, E.M., Sinninghe Damsté, J.S., Schouten, S., 2010. Glacial–interglacial variability in Atlantic meridional overturning circulation and thermocline adjustments in the tropical North Atlantic. Earth and Planetary Science Letters 300, 407–414.

Martens-Habbena W, Berube PM, Urakawa H, de la Torre JR, Stahl DA (2009) Ammonia oxidation kinetics determine niche separation of nitrifying Archaea and Bacteria. Nature 461, 7266, 976–979.

Miller, K. G., Wright, J. D., Browning, J. V., 2005. Visions of ice sheets in a greenhouse world. Marine Geology 217, 215-231. DOI: 10.1016/j.margeo.2005.02.007

Minard, J.P. 1969. Geology of the Sandy Hook quadrangle in Monmouth County, New Jersey. United States Geology Survey Bulletin 1276: 1–43.

Olsson, R. K., 1987. Cretaceous stratigraphy of the Atlantic Coastal Plain, Atlantic Highlands of New Jersey. Geological Society of America Centennial Field Guide-Northeastern Section: 87–90.

Olsson, R. K., Miller, K. G., Browning, J. V., Habib, D., Sugerman, P. J., 1997. Ejecta layer at the Cretaceous-Tertiary boundary, Bass River, New Jersey (Ocean Drilling Program Leg 174AX). Geology 25, 759-762.

Olsson R. K, Hemleben C, Berggren W. A., Huber B. T., Editors and Members of the Paleogene Planktonic Foraminifera Working Group, 1999. Atlas of Paleocene Planktonic Foraminifera. Smithsonian Contributions to Paleobiology 85, pp. 255.

Pardo, A., Keller, G., 2008. Biotic effects of environmental catastrophes at the end of the Cretaceous and early Tertiary: Guembelitria and Heterohelix blooms. Cretaceous Research 29, 1058-1073.

Premoli Silva I., Verga D., 2004. Practical Manual of Cretaceous Planktonic Foraminifera. International School on Planktonic Foraminifera. 3 Course: Cretaceous. Verga & Rettori eds Universities of Perugia and Milan, Tipografia Pontefelcino, Perugia (Italy), 283 p.

Qin W, et al., 2014. Marine ammonia-oxidizing archaeal isolates display obligate mixotrophy and wide ecotypic variation. Proc Natl Acad Sci USA 111(34):12504–12509.

Oin, W., et al. 2015. Confounding effects of oxygen and temperature on the $TEX_{86}$ signature of marine Thaumarchaeota. Proc Natl Acad Sci USA 112(35):10979–10984.

Ravizza, G., Pyle, D., 1997. PGE and Os isotopic analyses of single sample aliquots with NiS fire assay preconcentration. Chemical Geology 141, 251–268.

Schiøler, P., Wilson, G.J., 1993. Maastrichtian dinoflagellate zonation in the Dan Field, Danish North Sea. Review of Palaeobotany and Palynology 78, 321-351.

Schouten, S., Huguet, C., Hopmans, E.C., Kienhuis, M.V., Sinninghe-Damsté, J.S. (2007) Analytical methodology for TEX86 paleothermometry by high-performance liquid chromatography/atmospheric pressure chemical ionization-mass spectrometry. Anal Chem 79(7):2940–2944.

Sluijs, A., Brinkhuis, H., Schouten, S., Bohaty, S. M., John, C. M., Zachos, J. C., Reichart, G. J., Sinninghe-Damsté, J. S., Crouch, E. M., Dickens, G. R., 2007. Environmental precursors to rapid light carbon injection at the Palaeocene/Eocene boundary. Nature 450, 1218-1221.

Van Helmond, N. A. G. M., Sluijs, A., Reichart, G. J., Sinninghe-Damsté, J. S., Slomp, C. P., Brinkhuis, H., 2013. A perturbed hydrological cycle during Oceanic Anoxic Event 2. Geology 42, 123-126. DOI: 10.1130/G34929.1

Weijers, J. W. H., Schouten, S., Spaargaren, O. C., Sinninghe Damsté, J. S., 2006. Occurrence and distribution of tetraether membrane lipids in soils: Implications for the use of the $TEX_{86}$ proxy and the BIT index. Organic Geochemistry 37, 1680-1693.

Weijers, J.W.H., Lim, K.L.H., Aquilina, A. Sinninghe Damsté, J.S. Pancost, R.D., Biogeochemical controls on glycerol dialkyl glycerol tetraether lipid distributions in sediments characterized by diffusive methane flux. Geochem. Geoph. Geasys. 12, 10 (2011).

Wuchter, C., Schouten, S., Coolen, M.J.L., Sinninghe Damsté, J.S., 2004, Temperaturedependent variation in the distribution of tetraether membrane lipids of marine Crenarchaeota: Implications for TEX86 paleothermometry. Paleoceanography 19(4):PA4028.

Yancey, T.E., Guillemette, .N., Carbonate accretionary lapilli in distal deposits of the Chicxulub impact event. GSA Bulletin 120 (9/10), p. 1105-1118. doi: 10.1130/B26146.1

Zhang, Y.G. et al., Methane Index: A tetraether archaeal lipid biomarker indicator for detecting the instability of marine gas hydrates. Earth and Planet. Sc. Lett. 307, 525-534 (2011)

## FIGURE CAPTIONS

**Figure DR1**. A core photograph of the K-Pg boundary interval of the Meirs Farm core, with the Iridium record and fecal pellets per gram (Miller et al., 2010) and $TEX_{86}$ derived sea surface temperature record (this study). The range of the lowermost Danian marker taxon *Senoniasphaera* cf. *inornata* is indicated.

**Figure DR2**. Age-depth plot of Meirs Farm 1, based on dinocyst biostratigraphy. A) overview of the entire core. LO: Lowest Occurrence. HO: Highest Occurrence. B) detail of the K-Pg boundary. Uncertainties in absolute ages of biostratigraphic events are indicated. According to Vellekoop et al. (2014) and Açikalin et al. (2015), the total range of *Senoniaspahera* cf. *inornata* falls with planktic foraminiferal Zone P0. Therefore, on the basis of the range of this taxon, the equivalent of Zone P0 can be indicated (grey interval). Sedimentation rates are indicated in the figure.

**Figure DR3**. Stratigraphic correlation between the Meirs Farm, Search Farm, Fort Monmouth 3 cores. The ranges stratigraphic marker taxa of organic-walled dinoflagellate cyst are indicated per core. Iridium and fecal pellet concentrations of the Meirs Farm and Search Farm cores are from Miller et al., 2010. In all cores, the basal part of the Hornerstown Formation is characterized by an interval of green, intensely burrowed glauconitic sand (shaded green in this figure. $TEX_{86}$ and BIT-index records are presented per core.

**Figure DR4**. $TEX_{86}$ derived sea surface temperatures of all analyzed samples plotted against BIT-index values. This plot indicates that there is correlation between SST and BIT, signifying that our $TEX_{86}$ record may be biased by the input of soil organic matter (with associated archaeal tetraethers) in our samples. According to earlier recommendations (Weijers et al., 2006), all samples with a BIT-index exceeding the threshold of 0.3 were discarded.

**Figure DR5**. $TEX_{86}$ derived sea surface temperature record of the Meirs Farm core, absolute concentrations of isoprenoidal GDGTs (in ng/g sediment), GDGT-0/Crenarchaeol ratio, Methane index and BIT index. This plot shows that our $TEX_{86}$ SST record is not biased by input of GDGTs derived from soil bacteria or methanogenic or methanotrophic archaea.

## TABLE CAPTIONS

Table DR1. Sample overview of Meirs Farm 1

Table DR2. Sample overview of Search Farm 1

Table DR3. Sample overview of Fort Monmouth 3

Table DR4. Dinoflagellate cyst stratigraphic marker ranges of Meirs Farm 1

Table DR5. Dinoflagellate cyst stratigraphic marker ranges of Search Farm 1

Table DR6. Dinoflagellate cyst stratigraphic marker ranges of Fort Monmouth 3

Table DR7. Planktic foraminiferal stratigraphic marker ranges of Fort Monmouth 3

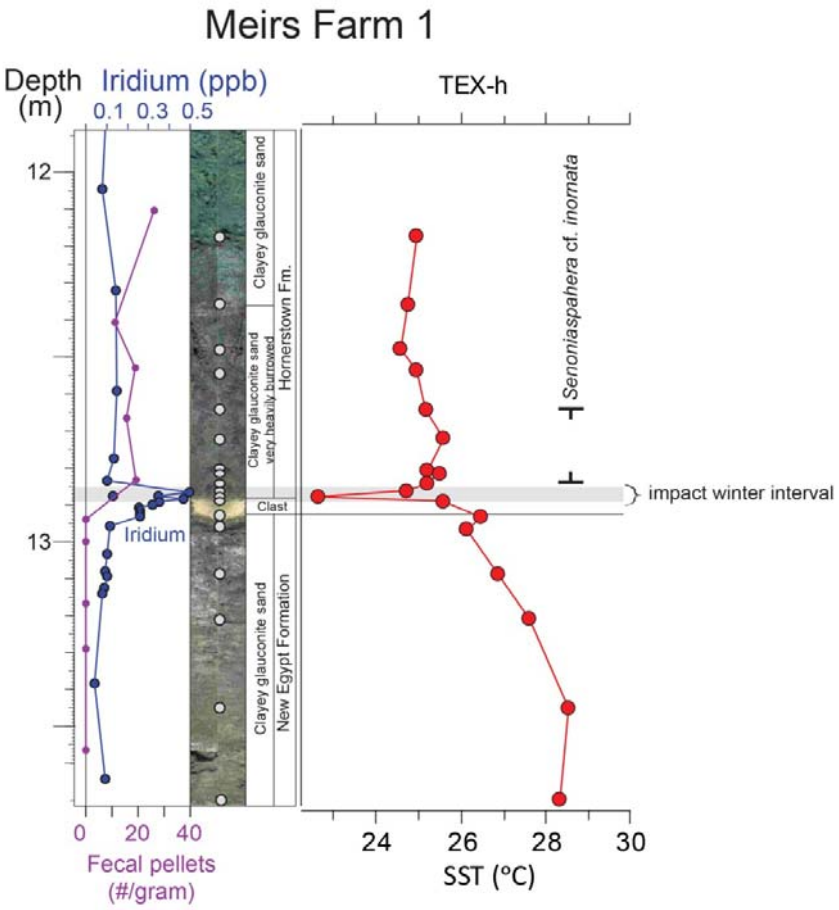
Meirs Farm 1
Depth (m)
Iridium (ppb)
0.1 0.3 0.5
12
13
Clayey glauconite sand
Hornerstown Fm.
Clayey glauconite sand
very heavily burrowed
Clast
Iridium
Clayey glauconite sand
New Egypt Formation
0 20 40
Fecal pellets (#/gram)
TEX-h
Senoniaspahera cf. inornata
impact winter interval
24 26 28 30
SST (°C)

Figure DR1

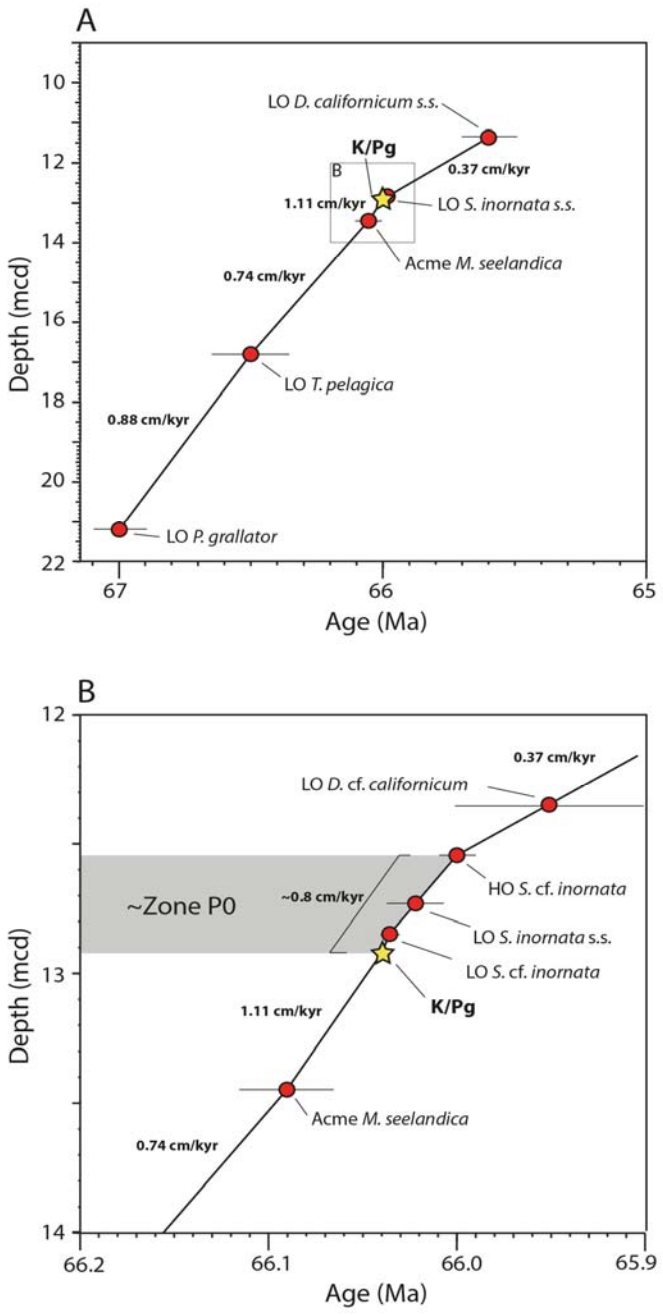
A
LO D. californicum s.s.
K/Pg
B
0.37 cm/kyr
1.11 cm/kyr
LO S. inornata s.s.
Acme M. seelandica
0.74 cm/kyr
LO T. pelagica
0.88 cm/kyr
LO P. grallator
Depth (mcd)
Age (Ma)
B
0.37 cm/kyr
LO D. cf. californicum
~Zone P0
~0.8 cm/kyr
HO S. cf. inornata
LO S. inornata s.s.
LO S. cf. inornata
K/Pg
1.11 cm/kyr
Acme M. seelandica
0.74 cm/kyr
Depth (mcd)
Age (Ma)

Figure DR2

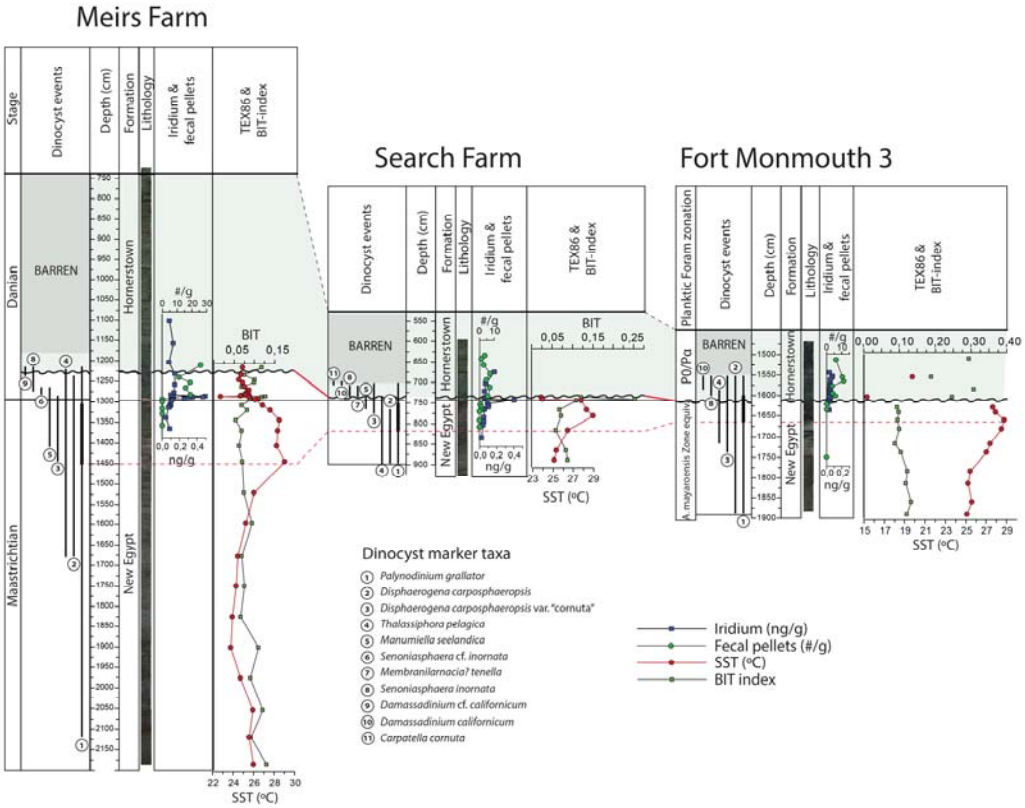
Meirs Farm
Search Farm
Fort Monmouth 3
Stage
Dinocyst events
Depth (cm)
Formation
Lithology
Iridium & fecal pellets
TEX86 & BIT-index
Planktic Foram zonation
Danian
Maastrichtian
BARREN
Hornerstown
New Egypt
P0/Pa
A. mayaroensis Zone equiv.
#/g
ng/g
BIT
SST (°C)
Dinocyst marker taxa
1 Palynodinium grallator
2 Disphaerogena carposphaeropsis
3 Disphaerogena carposphaeropsis var. "cornuta"
4 Thalassiphora pelagica
5 Manumiella seelandica
6 Senoniasphaera cf. inornata
7 Membranilarnacia? tenella
8 Senoniasphaera inornata
9 Damassadinium cf. californicum
10 Damassadinium californicum
11 Carpatella cornuta
Iridium (ng/g)
Fecal pellets (#/g)
SST (°C)
BIT index

Figure DR3

Figure DR4

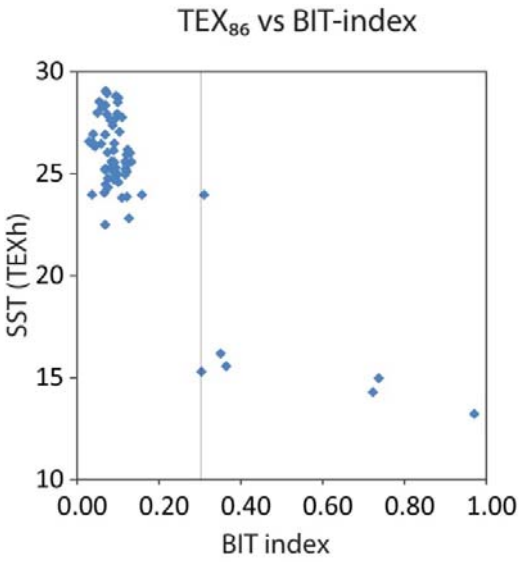
TEX86 vs BIT-index
SST (TEXh)
30
25
20
15
10
0.00
0.20
0.40
0.60
0.80
1.00
BIT index

Figure DR5

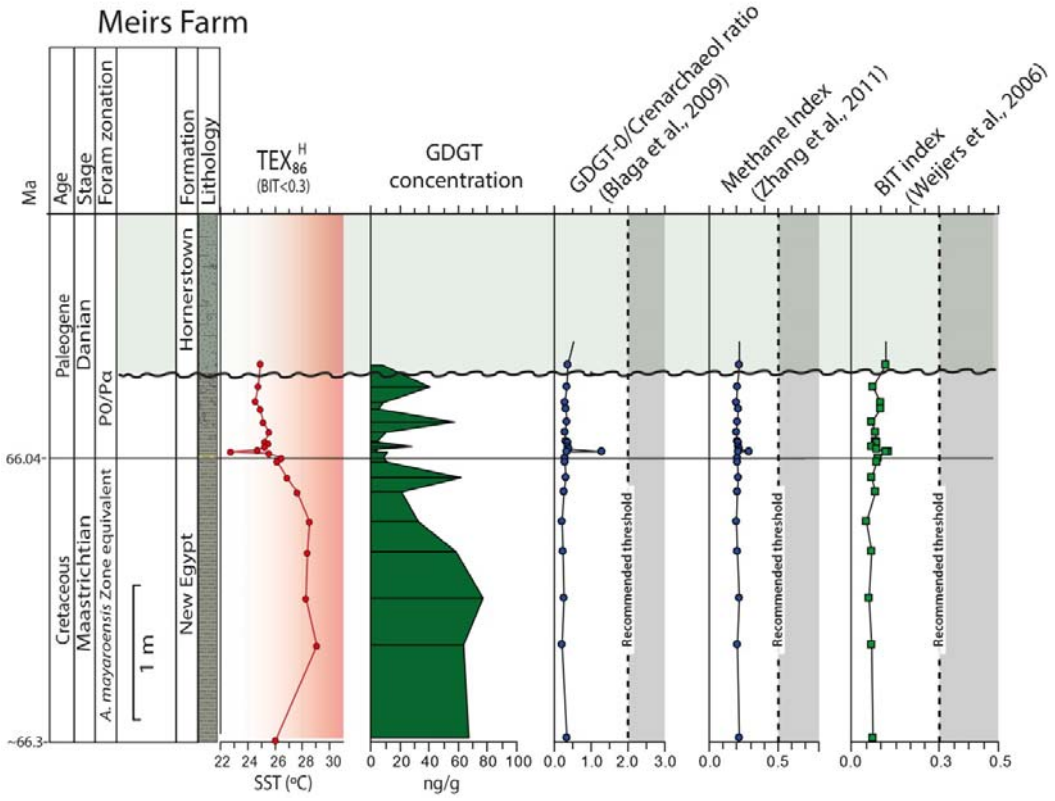
Meirs Farm
Ma
Age
Stage
Foram zonation
Formation
Lithology
TEX86H
(BIT<0.3)
GDGT concentration
GDGT-0/Crenarchaeol ratio (Blaga et al., 2009)
Methane Index (Zhang et al., 2011)
BIT index (Weijers et al., 2006)
Paleogene
Danian
P0/Pα
Hornerstown
66.04
Cretaceous
Maastrichtian
A. mayaroensis Zone equivalent
1 m
New Egypt
~66.3
Recommended threshold
Recommended threshold
Recommended threshold
22 24 26 28 30
SST (°C)
0 20 40 60 80 100
ng/g
0.0 1.0 2.0 3.0
0.0 0.5
0.0 0.3 0.5

Table DR1

| MEIRS FARM | | | | | | |
|---|---|---|---|---|---|---|
| Depth interval (ft) | Depth midpoint (ft) | Depth midpoint (cm) | Palynology | TEX86-based SST | BIT | Comments |
| | | | | | | |
| 24.0 - 24.1 | 24.05 | 733.0 | X | | | Poor organic matter preservation |
| 27.3 - 27.4 | 27.35 | 833.6 | X | | | Poor organic matter preservation |
| 29.4 - 29.5 | 29.45 | 897.6 | X | | | Poor organic matter preservation |
| 32.4 - 32.5 | 32.45 | 989.1 | X | | | Poor organic matter preservation |
| 34.9 - 35.0 | 34.95 | 1065.3 | X | | | Poor organic matter preservation |
| 37.4 - 37.5 | 37.45 | 1141.5 | X | 13.2 | 0.97 | Poor organic matter preservation |
| 39.9 - 40.0 | 39.95 | 1217.7 | X | 25.0 | 0.12 | |
| 40.5 - 40.6 | 40.55 | 1236.0 | X | 24.8 | 0.08 | |
| 40.9 - 41.0 | 40.95 | 1248.2 | X | 24.6 | 0.10 | |
| 41.1 - 41.2 | 41.15 | 1254.3 | X | 25.0 | 0.10 | |
| 41.45 - 41.5 | 41.475 | 1264.2 | X | 25.2 | 0.07 | |
| 41.7 - 41.8 | 41.75 | 1272.5 | X | 25.6 | 0.08 | |
| 42.0 - 42.05 | 42.025 | 1280.9 | X | 25.2 | 0.08 | |
| 42.05 - 42.10 | 42.075 | 1282.4 | X | 25.5 | 0.09 | |
| 42.12 - 42.18 | 42.15 | 1284.7 | X | 25.2 | 0.07 | |
| 42.2 - 42.25 | 42.225 | 1287.0 | X | 24.7 | 0.09 | |
| 42.3 - 42.35 | 42.325 | 1290.1 | X | 22.8 | 0.13 | |
| 42.25 - 42.31 | 42.28 | 1288.7 | | 25.6 | 0.12 | To little material for palynology |
| 42.4 - 42.5 | 42.45 | 1293.9 | X | 26.5 | 0.09 | |
| 42.5 - 42.6 | 42.55 | 1296.9 | X | 26.1 | 0.09 | |
| 42.95 - 43.0 | 42.975 | 1309.9 | X | 26.9 | 0.07 | |
| 43.3 - 43.4 | 43.35 | 1321.3 | X | 27.6 | 0.08 | |
| 44.1 - 44.2 | 44.15 | 1345.7 | X | 28.5 | 0.05 | |
| 44.9 - 45.0 | 44.95 | 1370.1 | X | 28.4 | 0.07 | |
| 46.18 - 46.22 | 46.2 | 1408.2 | X | 28.3 | 0.06 | |
| 47.4 - 47.5 | 47.45 | 1446.3 | X | 29.1 | 0.07 | |
| 49.9 - 49.95 | 49.975 | 1523.2 | X | 26.0 | 0.07 | |
| 52.4 - 52.5 | 52.45 | 1598.7 | X | 25.3 | 0.09 | |
| 55.05 - 55.1 | 55.075 | 1678.7 | X | 24.5 | 0.07 | |
| 57.4 - 57.5 | 57.45 | 1751.1 | X | 24.3 | 0.08 | |
| 59.9 - 59.95 | 59.925 | 1826.5 | X | 24.1 | 0.07 | |
| 62.5 - 62.6 | 62.55 | 1906.5 | X | 23.8 | 0.11 | |
| 64.95 - 65.0 | 64.975 | 1980.4 | X | 24.7 | 0.09 | |
| 67.4 - 67.5 | 67.45 | 2055.9 | X | 25.9 | 0.12 | |
| 69.55 - 69.6 | 69.575 | 2120.6 | X | 25.6 | 0.09 | |
| 71.7 - 71.8 | 71.75 | 2186.9 | X | 26.0 | 0.13 | |
| | | | | | | |

Table DR2

| SEARCH FARM | | | | | | |
|---|---|---|---|---|---|---|
| Depth interval (ft) | Depth midpoint (ft) | Depth midpoint (cm) | Paly nolo gy | TE X86 - base d SST | BIT | Comments |
| | | | | | | |
| 20.3 - 20.4 | 20.35 | 620.3 | X | | | |
| 21.3 - 21.4 | 21.35 | 650.7 | X | 15.0 | 0.74 | Poor organic matter preservation |
| 23.3 - 23.4 | 23.35 | 711.7 | X | 14.3 | 0.72 | Poor organic matter preservation |
| 24.0 - 24.1 | 24.05 | 733.0 | X | 23.9 | 0.12 | |
| 24.2 - 24.25 | 24.225 | 738.4 | X | 24.0 | 0.25 | |
| 24.3 - 24.35 | 24.325 | 741.4 | X | 27.8 | 0.11 | |
| 24.55 - 24.6 | 24.575 | 749.0 | X | | | To little material to analyze for OG |
| 24.85 - 24.8 | 24.875 | 758.2 | X | | | |
| 25.0 - 25.1 | 25.05 | 763.5 | X | 28.3 | 0.07 | |
| 25.5 - 25.6 | 25.55 | 778.8 | X | 28.9 | 0.07 | |
| 26.6 - 26.7 | 26.65 | 812.3 | X | 26.5 | 0.06 | |
| 28.2 - 28.3 | 28.25 | 861.1 | X | 25.3 | 0.08 | |
| 29.0 - 29.1 | 29.05 | 885.4 | X | 25.1 | 0.09 | |
| | | | | | | |

Table DR3

| FORT MONMOUTH 3 | | | | | | | | |
|---|---|---|---|---|---|---|---|---|
| Depth interval (ft) | Depth midpoint (ft) | Depth midpoint (cm) | Palynology | TEX86-based SST | BIT | Forams | Iridium (ng/g) | Comments |
| | | | | | | | | |
| 49.5 - 49.6 | 49.55 | 1510.3 | X | 16.2 | 0.29 | | | Poor organic matter preservation |
| 49.6 - 49.7 | 49.65 | 1513.3 | | | | X | | |
| 50.6 - 50.7 | 50,65 | 1543,8 | | | | | 0,03790 | |
| 50.9 - 51.0 | 50,95 | 1553,0 | | | | | 0,07994 | |
| 51.00 -51.05 | 51.025 | 1555.2 | | | | X | | |
| 51.0 - 51.1 | 51.05 | 1556.0 | X | 19.8 | 0.19 | | 0,07277 | |
| 51.2 - 51.3 | 51,25 | 1562,1 | | | | | 0,04602 | |
| 51.35 - 51.40 | 51.375 | 1565.9 | | | | X | | |
| 51.45 - 51.55 | 51,5 | 1569,7 | | | | | 0,04839 | |
| 51.60 - 51.65 | 51.625 | 1573.5 | | | | X | | |
| 51.6 - 51.7 | 51,65 | 1574,3 | | | | | 0,04805 | |
| 51.7 - 51.8 | 51,75 | 1577,3 | | | | | 0,05036 | |
| 51.75 - 51.80 | 51.775 | 1578.1 | | | | X | | |
| 51.85 - 51.95 | 51,9 | 1581,9 | | | | | 0,04325 | |
| 52.0 - 52.1 | 52.05 | 1586.5 | X | 15.6 | 0.31 | | 0,05159 | |
| 52.15 - 52.25 | 52,2 | 1591,1 | | | | | 0,04442 | |
| 52.25 - 52.35 | 52,3 | 1594,1 | | | | | 0,04998 | |
| 52.3 - 52.4 | 52.35 | 1595.6 | | | | X | | |
| 52.4 - 52.5 | 52,45 | 1598,7 | | | | | 0,05162 | |
| 52.55 - 52.60 | 52.575 | 1602.5 | | | | X | | |
| 52.55 - 52.65 | 52,6 | 1603,2 | | | | | 0,02961 | |
| 52.60 - 52.65 | 52.625 | 1604.0 | | | | X | | |
| 52.6 - 52.7 | 52.65 | 1604.8 | X | 15.3 | 0.25 | | | |
| 52.80 - 52.85 | 52.825 | 1610.1 | | | | X | | |
| 52.8 - 52.9 | 52,85 | 1610,9 | | | | | 0,04627 | |
| 52.85 - 52.9 | 52.875 | 1611.6 | X | | | | | |
| 52.95 - 53.00 | 52.975 | 1614.7 | | | | X | | |
| 52.95 – 53.05 | 53.0 | 1615,4 | | | | | 0,03785 | |
| 53.2 - 53.3 | 53.25 | 1623.0 | | | | X | | |
| 53.4 - 53.5 | 53.45 | 1629.2 | X | 27.7 | 0.09 | | | |
| 53.6 - 53.7 | 53.65 | 1635.3 | | | | X | 0,03687 | |
| 53.8 - 53.9 | 53.85 | 1641.3 | X | 27.9 | 0.10 | | | |
| 54.4 - 54.5 | 54.55 | 1662.7 | X | 28.8 | 0.10 | | | |
| 55.1 - 55.2 | 55.15 | 1681.0 | X | 28.5 | 0.10 | | | |
| 56.3 - 56.4 | 56.35 | 1717.5 | X | 27.4 | 0.09 | | | |
| 57.00 - 57.10 | 57.05 | 1738.9 | X | 27.0 | 0.10 | | | |
| 57.4 - 57.5 | 57.45 | 1751.1 | | | | X | | |
| 58.5 58.6 | 58.55 | 1784.6 | X | 25.4 | 0.12 | | | |
| 59.5 - 59.6 | 59.55 | 1815.1 | X | 25.2 | 0.12 | | | |
| 61.00 - 61.10 | 61.05 | 1860.8 | X | 25.6 | 0.13 | | | |
| 62.00 - 62.10 | 62.05 | 1891.3 | X | 25.1 | 0.12 | | | |
| | | | | | | | | |

Table DR4

| MEIRS FARM | | | | | | | | | | | |
|---|---|---|---|---|---|---|---|---|---|---|---|
| Depth interval (ft) | Depth midpoint (ft) | Depth midpoint (cm) | P. grallator | D. carposphaeropsis | *T. pelagica* | D. carpo. "comuta" | M. seelandica | M.? tenella | S. cf. inornata | S. inornata | D. cf. californicum |
| | | | | | | | | | | | |
| 24.0 - 24.1 | 24.05 | 733.0 | | | | | | | | | |
| 27.3 - 27.4 | 27.35 | 833.6 | | | | | | | | | |
| 29.4 - 29.5 | 29.45 | 897.6 | | | | | | | | | |
| 32.4 - 32.5 | 32.45 | 989.1 | | | | | | | | | |
| 34.9 - 35.0 | 34.95 | 1065.3 | | | | | | | | | |
| 37.4 - 37.5 | 37.45 | 1141.5 | | | | | | | | | |
| 39.9 - 40.0 | 39.95 | 1217.7 | X | | | | | | | X | X |
| 40.5 - 40.6 | 40.55 | 1236.0 | X | X | x | | | | | X | X |
| 40.9 - 41.0 | 40.95 | 1248.2 | X | | | | | | | X | |
| 41.1 - 41.2 | 41.15 | 1254.3 | X | | | | | | | X | |
| 41.45 - 41.5 | 41.475 | 1264.2 | X | | x | | X | | X | X | |
| 41.7 - 41.8 | 41.75 | 1272.5 | X | | | | | | | X | |
| 42.0 - 42.05 | 42.025 | 1280.9 | X | X | | | X | X | | | |
| 42.05 - 42.10 | 42.075 | 1282.4 | X | X | | | | X | | | |
| 42.12 - 42.18 | 42.15 | 1284.7 | X | X | | X | | | X | | |
| 42.2 - 42.25 | 42.225 | 1287.0 | X | X | | | | X | | | |
| 42.3 - 42.35 | 42.325 | 1290.1 | X | | | | | | | | |
| 42.4 - 42.5 | 42.45 | 1293.9 | X | X | | | X | | | | |
| 42.5 - 42.6 | 42.55 | 1296.9 | XX | X | x | X | X | | | | |
| 42.95 - 43.0 | 42.975 | 1309.9 | XX | X | x | | X | | | | |
| 43.3 - 43.4 | 43.35 | 1321.3 | XX | X | x | X | | | | | |
| 44.1 - 44.2 | 44.15 | 1345.7 | XX | X | x | X | X | | | | |
| 44.9 - 45.0 | 44.95 | 1370.1 | XX | X | x | X | X | | | | |
| 46.18 - 46.22 | 46.2 | 1408.2 | XX | X | | | X | | | | |
| 47.4 - 47.5 | 47.45 | 1446.3 | XX | X | | X | | | | | |
| 49.9 - 49.95 | 49.975 | 1523.2 | X | X | | | | | | | |
| 52.4 - 52.5 | 52.45 | 1598.7 | X | | x | | | | | | |
| 55.05 - 55.1 | 55.075 | 1678.7 | X | X | x | | | | | | |
| 57.4 - 57.5 | 57.45 | 1751.1 | X | | | | | | | | |
| 59.9 - 59.95 | 59.925 | 1826.5 | X | | | | | | | | |
| 62.5 - 62.6 | 62.55 | 1906.5 | X | | | | | | | | |
| 64.95 - 65.0 | 64.975 | 1980.4 | X | | | | | | | | |
| 67.4 - 67.5 | 67.45 | 2055.9 | X | | | | | | | | |
| 69.55 - 69.6 | 69.575 | 2120.6 | X | | | | | | | | |
| 71.7 - 71.8 | 71.75 | 2186.9 | | | | | | | | | |
| | | | | | | | | | | | |

Table DR5

| SEARCH FARM | | | P. grallator | D. carposphaeropsis | T. pelagica | D. carpo. "cornuta" | M. seelandica | M.? tenella | S. inornata | D. californicum | C. cornuta |
|---|---|---|---|---|---|---|---|---|---|---|---|
| Depth interval (ft) | Depth midpoint (ft) | Depth midpoint (cm) | | | | | | | | | |
| | | | | | | | | | | | |
| 20.3 - 20.4 | 20.35 | 620.3 | | | | | | | | | |
| 21.3 - 21.4 | 21.35 | 650.7 | | | | | | | | | |
| 23.3 - 23.4 | 23.35 | 711.7 | X | | | X | | | X | X | X |
| 24.0 - 24.1 | 24.05 | 733.0 | X | | X | X | | X | X | | |
| 24.2 - 24.25 | 24.225 | 738.4 | X | | X | | X | | | | |
| 24.3 - 24.35 | 24.325 | 741.4 | X | | X | X | | | | | |
| 24.55 - 24.6 | 24.575 | 749.0 | XX | | X | X | X | | | | |
| 24.85 - 24.8 | 24.875 | 758.2 | XX | | X | X | | | | | |
| 25.0 - 25.1 | 25.05 | 763.5 | XX | X | X | X | X | | | | |
| 25.5 - 25.6 | 25.55 | 778.8 | XX | | X | X | | | | | |
| 26.6 - 26.7 | 26.65 | 812.3 | XX | X | X | | | | | | |
| 28.2 - 28.3 | 28.25 | 861.1 | X | | | | | | | | |
| 29.0 - 29.1 | 29.05 | 885.4 | X | X | X | | | | | | |
| | | | | | | | | | | | |

Table DR6

| FORT MONMOUTH 3 | | | | | | | | | |
|---|---|---|---|---|---|---|---|---|---|
| Depth interval (ft) | Depth midpoint (ft) | Depth midpoint (cm) | P. grallator | D. carposphaeropsis | D. carpo. "cornuta" | T. pelagica | S. inornata | D. californicum | |
| | | | | | | | | | |
| 49.5 - 49.6 | 49.55 | 1510.3 | | | | | | | |
| 51.0 - 51.1 | 51.05 | 1556.0 | X | X | X | | X | X | |
| 52.0 - 52.1 | 52.05 | 1586.5 | X | X | X | | | X | |
| 52.6 - 52.7 | 52.65 | 1604.8 | XX | X | X | X | X | | |
| 52.85 - 52.9 | 52.875 | 1611.6 | XX | X | X | X | | | |
| 53.4 - 53.5 | 53.45 | 1629.2 | XX | X | X | | | | |
| 53.8 - 53.9 | 53.85 | 1641.3 | XX | X | X | | | | |
| 54.4 - 54.5 | 54.55 | 1662.7 | X | X | X | X | | | |
| 55.1 - 55.2 | 55.15 | 1681.0 | X | | | X | | | |
| 56.3 - 56.4 | 56.35 | 1717.5 | X | X | | X | | | |
| 57.00 - 57.10 | 57.05 | 1738.9 | X | X | X | | | | |
| 58.5 58.6 | 58.55 | 1784.6 | X | | | | | | |
| 59.5 - 59.6 | 59.55 | 1815.1 | X | | | | | | |
| 61.00 - 61.10 | 61.05 | 1860.8 | X | | | | | | |
| 62.00 - 62.10 | 62.05 | 1891.3 | X | X | | | | | |
| | | | | | | | | | |

Table DR7

| FORT MONMOUTH 3 | | | | | | | | | | | | | |
|---|---|---|---|---|---|---|---|---|---|---|---|---|---|
| Depth interval (ft) | Depth midpoint (ft) | Depth midpoint (cm) | G. praiehillensis | G. messinae | G. cretacea | H. navarroensis | H. globulosa | H.holmdelensis | Heterohelix sp. | H. planata (?) | Globigerinelloides sp. | COMMENTS |
| | | | | | | | | | | | | |
| 49.6 - 49.7 | 49.65 | 1513.3 | | | XX | X | X | | | X | X | G. cretacea is abundant |
| 51.00 -51.05 | 51.025 | 1555.2 | | | | | | | | | | No forams |
| 51.35 - 51.40 | 51.375 | 1565.9 | | | | | | | X | | | Forams rare |
| 51.60 - 51.65 | 51.625 | 1573.5 | | | | | | | | | | No forams |
| 51.75 - 51.80 | 51.775 | 1578.1 | | | | | | | | | | No forams |
| 52.3 - 52.4 | 52.35 | 1595.6 | | | X | X | X | | | | | |
| 52.55 - 52.60 | 52.575 | 1602.5 | | | | | | | | | | No forams |
| 52.60 - 52.65 | 52.625 | 1604.0 | | | | | | | | | | No forams |
| 52.80 - 52.85 | 52.825 | 1610.1 | | | | | | | | | | No forams |
| 52.95 - 53.00 | 52.975 | 1614.7 | | | | | | | | | | No forams |
| 53.2 - 53.3 | 53.25 | 1623.0 | | | X | | X | X | | | | |
| 53.6 - 53.7 | 53.65 | 1635.3 | | | | | X | | | | | Forams rare |
| 57.4 - 57.5 | 57.45 | 1751.1 | X | X | X | X | X | | | | | |
| | | | | | | | | | | | | |